Molecular & Cellular Toxicology (2021) 17:245–256
https://doi.org/10.1007/s13273-021-00131-y

ORIGINAL ARTICLE

OSI-027 alleviates rapamycin insensitivity by modulation of mTORC2/AKT/TGF-β1 and mTORC1/4E-BP1 signaling in hyperoxia-induced lung injury infant rats

Li Long[1] · Mulin Liang[2,5] · Yanling Liu[3,4,5] · Pan Wang[3,4,5] · Hongxing Dang[3,4,5]

Accepted: 5 March 2021 / Published online: 1 April 2021

Abstract

Background The mechanism of long time and high-concentration oxygen treatment leading to acute lung injury (ALI) or developmental lung disease in infants is currently unclear. Here we found that compared with the effect of rapamycin, pan-mTOR1/2 inhibitor OSI-027, alleviates hyperoxia-induced lung injury (HILI) by modulation of mTORC2/AKT/TGF-β1 and mTORC1/4E-BP1 signaling in infant rats.

Objective Infant rats were treated with continuous inhalation of 90% medical oxygen. Normal saline, rapamycin, or OSI-027 was intraperitoneally injected, and the status of lung injury was tested on days 3, 7, and 14. The activation of mTOR/AKT/TGFβ1 and mTORC1/4E-BP1 signaling was confirmed by immunohistochemistry and Western blot analysis in normal and hyperoxia-treated live precision-cut lung tissues. The inhibitory effect of OSI-027 extended to the active state of other proteins implicated in mTOR1/2 signaling was demonstrated in hyperoxia-induced injured lung tissues.

Results Our data demonstrate that hyperoxia-induced serious lung inflammation and fibrosis. OSI-027 significantly attenuated the pathological process of HILI, inhibit the phosphorylation of the primary downstream targets of mTORC1/C2, and reduce the activation of TGF-β1 signaling.

Conclusions The results suggest that mTORC2/AKT/TGF-β1 and the rapamycin-insensitive mTORC1/4E-BP1 (Thr37/46) signaling has an important effect during HILI with a potential meaning for the progress of novel anti-hyperoxia-injury strategies.

Keywords Hyperoxia · Lung injury · Rapamycin · OSI-027 · MTOR

Li Long and Mulin Liang make equal contributions to this study.

✉ Hongxing Dang
danghx@hospital.cqmu.edu.cn

Li Long
472860963@qq.com

Mulin Liang
mulinliang@qq.com

Yanling Liu
liuyanling1990@163.com

Pan Wang
panwang0908@163.com

[1] Health Management Center, The First Affiliated Hospital of Chongqing Medical University, Chongqing 400016, China

[2] Department of Neonatology, The Fifth Affiliated Hospital of Southern Medical University, Guangzhou 510900, China

[3] Ministry of Education Key Laboratory of Child Development and Disorders, Chongqing 400014, China

[4] China International Science and Technology Cooperation Base of Child Development and Critical Disorders, Chongqing 400014, China

[5] Department of PICU, Children's Hospital of Chongqing Medical University, 136 Zhongshan No. 2 Road, Yu Zhong District, Chongqing 400014, China

Introduction

Oxygen treatment is a common therapeutic strategy for critical respiratory and circulatory diseases, especially in infants (Reyburn et al. 2012; Kallet and Matthay 2013). In clinical practice, it is difficult to avoid oxygen therapy for a long time and at a high concentration, potentially leading to acute lung injury (ALI) or lung developmental disorders and even death (Helmerhorst et al. 2015). It is also one of the main etiological factors of pulmonary fibrosis (Vogel et al. 2015). Unfortunately, owing to the lack of effective treatments, current therapies for hyperoxia-induced lung injury (HILI) at best provide symptomatic relief. HILI and bronchopulmonary dysplasia are still major causes of mortality and morbidity among some infants (Higgins et al. 2018).

HILI is manifested as inflammatory exudation, edema, and alveolar damage in lung tissues in the early stage and lung interstitial fibrosis and alveolar obstruction in the later stage. Accordingly, a potential strategy for the alleviation of lung injury and fibrosis is the negative regulation of the inflammatory process and lung fiber cell proliferation.

The mTOR signaling pathway is involved in the expression of collagen, cell cycle control, cell survival, and proliferation. Furthermore, it plays an important role in the repair of tissue damage and the development of fibrosis. The inhibition of the mTOR signaling pathway has potential therapeutic effects on lung injury and fibrosis (Hu et al. 2014), but the specific mechanism underlying these effects is unclear now.

Rapamycin by indication a complex with its cellular receptor FKBP12 (a 12 kDa binding protein of FK506) to carried out its activity that blocks the interaction between mTORC1 (evolvingly conserved serine/threonine kinase) and regulatory proteins (Yang et al. 2017). It is widely used in anti-rejection treatment after transplantation (Hamdani et al. 2017). Due to its effective immunosuppressive activity and decreasing toxicity, rapamycin has being used to treat lung injury in many researches, but rapamycin has shown controversial roles in this field excepted for its immunosuppressive effect (Nadon et al. 2014; Segura-Ibarra et al. 2017; Dejust et al. 2018). OSI-027 is a novel selective and potent dual inhibitor of mTORC1 and mTORC2, and more than 100-fold selectivity observed for mTOR than PI3Kα, PI3Kβ, PI3Kγ or DNA-PK (Bahrami et al. 2018). In addition, OSI-027 exhibits anti-proliferative activities against several acute leukemia cell lines of myeloid/megakaryocytic origin in a dose-dependent manner (Gupta et al. 2012). OSI-027 has also attracted interest due to its competition with ATP in mTOR kinase activity in solid tumor (Tian et al. 2019).

In this study, we characterize two proprietary inhibitors and separately use them in 3-week-old SD rats for dephosphorylation of the mechanism by which the mTOR inhibition blocks TGF-β1 in lung injury induced by hyperoxia. The study shed light on the signaling pathways by which AKT/TGF-β1 and mTORC1/4E-BP1 exert their potent function on HILI effects in infant rats and provides support for targeting mTORC1/2 signaling selectively in HILI and potentially other same status.

Materials and methods

Experimental animals

A total of 72 healthy infant specific-pathogen-free Sprague–Dawley rats (weighing 50.6 ± 4.48 g; age 21 days, 1:1 ratio of males to females) were obtained from the Experimental Animal Center from Chongqing Medical University (Chongqing, China). Infancy is a general term. it is the nursing period, from birth to 42 days (Andreollo et al. 2012). After 18 days from born, a rat can intake water, On 21 days, infant rats can be weaned and eat solid food, then can be separated from the mother rat (Ošťádalová and Babický 2012), used in the experiment. we choose a rat of 21 days age in this study, close to a human infant.

Antibodies and materials

Primary antibodies: mTOR antibody (ab134903), Phospho-Smad3 (Ser423/425), antibody (1880-1), β-actin (ab8226) were obtained from Abcam (Cambridge, United Kingdom). Phospho-Akt (Ser473) antibody (#4060), Akt (pan) antibody (#4691), TGF-β1 antibody (#3709), Phospho-Smad2 (Ser465/467) antibody (#3108), Smad2 antibody (#5339), Smad3 antibody (#9523), Phospho-4E-BP1 (Thr37/46) antibody (#2855), Phospho-4E-BP1 (Ser65) antibody (#9451), 4E-BP1antibody (#9644), Phospho-p70S6k Kinase (Thr389) antibody (#9206), p70S6k Kinase antibody (#2708) were purchased from Cell Signaling Technology (Beverly, MA, United State). LAP (Latency Associated peptide) Monoclonal Antibody was obtained from Invitrogen (#16-9823-82).

Secondary antibodies: HRP conjugated anti-rabbit (mouse, and goat) IgG, were purchased from Abcam (Cambridge, UK). Goat serum (ZLI-9021), and the Rat Disabled Homolog (DAB) ELISA Kit (K135925C) were purchased from Zsbio (Beijing, China). Rapamycin (R8140) was purchased from Solarbio (Beijing, China). OSI-027 (HY-10423/CS-0257) was purchased from Med Chem Express (Monmouth Junction, NJ, USA). The Tissue Total Protein Extraction Kit (KGP2100) and BCA Protein Assay Kit (KGP903) were purchased from KeyGen Biotech (Nanjing, China). Prestained Color Protein Marker (00215343) was purchased from New England Biolabs (Ipswich, MA, USA).

The Enhanced Chemiluminescent Kit was purchased from Thermo (Waltham, MA, USA).

Animal groups and hyperoxic model preparation

A total of 72 infant rats were randomly assigned to the following four groups using a random number table: group A, Normoxia + normal saline; group B, Hyperoxia + normal saline; group C, Hyperoxia + rapamycin; and group D, Hyperoxia + OSI-027 ($n = 18$ per group). There were no significant differences in weight among the four groups. The rat model of HILI originally created by our research team was used.

Each group of infant rats of equal weight was nested on cork shavings and distributed into each plexiglass chamber. These chambers were equipped with a flow system to control the delivery of indoor air or medical oxygen. food and water were provided and lighting during a 12-h light–dark cycle. The temperature of the rooms and chamber were maintained at 22–24 °C.

The oxygen concentration in room air was maintained at 21 ± 2%, and this was provided by group A. The other three hyperoxia intervention groups were provided 6 l/min medical oxygen, which was allowed to flow through the chambers under continuous monitoring using a digital oxygen meter, maintaining inhaling oxygen concentrations of 90 ± 2%. Sodium lime was used to absorb CO_2, and the CO_2 concentration was maintained at less than 0.5%. The relative humidity was maintained at 60–80%.

With respect to drug interventions, infant rats in groups A and B received 0.5 ml of normal saline as a control for intraperitoneal microinjection. Groups C and D were intraperitoneally microinjected with rapamycin (1.5 mg kg^{-1} day^{-1}) and OSI-027 (0.5 mg kg^{-1} day^{-1}). Both drugs were diluted to an overall volume of 0.5 ml in normal saline. The drugs were regularly administered at 10 am on days 1, 3, 6, 8, 10, and 13 of the experiment. All infant rats were exposed to air for 1 h after each intraperitoneal microinjection and were then exposed to the corresponding hyperoxic or normoxic conditions.

The general status of the animals, including autonomous activity, diet, reaction to stimulation, the luster of body hair, breathing condition (with or without shortness of breath), and weight changes, were recorded every day during the experiment.

Specimens

SD infant rats ($n = 6$) in each group were sacrificed after the administration of anesthesia by the intraperitoneal injection of pentobarbital sodium (150 mg/kg) on days 3, 7, and 14. The rats were fully anesthetized by observing the nonresponse to stimulate its tail and determined the rats were not euthanized by observing the rats' normal breathing. The rats were fully anesthetized and without any symptoms of peritonitis were observed after 4 min of intraperitoneal injection of pentobarbital sodium. At last, euthanasia was performed with cervical dislocation, and the rats had sacrificed by observing the cardiac arrest. Then, the chest was opened and lung tissue samples were collected. First, the right lung main bronchus was ligated near the main trachea, and the whole right lung was subsequently extracted from the distal end of the ligation site. The right middle and upper lung lobes were resectioned, snap-frozen in liquid nitrogen, and stored at − 80 °C for further protein biochemical analysis. The lung wet/dry weight (*W/D*) ratio was measured in the right lower lobe. Second, the left lung was perfused with 4% paraformaldehyde for 10 min under a constant airway pressure of 10 cmH_2O, which was maintained via a tracheal tube. After the left lung was excised and fixed by overnight immersion in 4% paraformaldehyde at 4 °C, these specimens were dehydrated in a graded ethanol series and embedded in paraffin for lung histopathological and immunohistochemical examinations.

Determination of lung *W/D*

The lower right lung lobe was placed on an absorbent filter paper to dry the blood on the surface. The sample was weighed immediately using an analytical balance to obtain the wet weight. The dry lung weight was obtained after placing the wet lung in an oven at 70 °C for 48 h. Then, the *W/D* weight ratio was calculated.

Lung histological examination

Five-micrometer-thick slices were cut from paraffin blocks of left lung tissues and stained with hematoxylin and eosin (HE) for general morphological analysis. Magnified digital images were captured using an Olympus BX40 microscope. The official American Thoracic Society workshop report: features and measurements of experimental acute lung injury in animals (Matute-Bello et al. 2011) was employed to grade the degree of lung tissue injury. The following were provided for histological assessment of features: A. Infiltration of neutrophils into alveolar cavities; B. Interstitial neutrophil infiltration; C. transparent film; D. exudation of protein fragments in alveolar cavities; E. thickening of alveolar interval. 20 fields were observed in each section, lung injury score = [20 x + 14 (A) × (C) (B) + 7 + 7 × (D) + 2 × (E)]/(views × 100). A total score for each subject was calculated. To eliminate bias and standardize the analyses, lung sections were collected from the central areas of the superior lobe of the left lung tissue, and a morphometric analysis of each slice was carried out in a blinded situation by two independent technicians.

The Image-pro Plus 6.0 image analysis system (US Media Cybernetics, Rockville, MD, USA) was used to measure the thickness of alveolar intervals 400 times. Then, fields were observed in each section, and 3 different alveolar walls were randomly measured in each field. The average value was taken as the thickness of the alveolar interval.

Immunochemistry

Left lung tissues were processed by immunohistochemistry with antibodies against mTOR (1:200), p-AKT1 (1:100), and TGF-β1 (1:200). The lung sections were de-paraffinized, re-hydrated with de-ionized water, and washed three times with phosphate-buffered saline. They were then incubated overnight at 4 °C with the primary antibodies. Sections were washed with phosphate-buffered saline and incubated with secondary antibodies at 37 °C for 30 min. After washing again, sections were incubated with 0.05% (w/v) 3,3-diaminobenzidine tetrahydrochloride dehydrate, counterstained with hematoxylin, dehydrated, and mounted for microscopic examination.

Positive cells were those in which the nuclei and/or cytoplasm appeared brownish-yellow or tan. Ten fields were randomly selected for each section, and three plots were selected for each field. Each plot was divided into 3–4 cells by staining.

Images were captured at a magnification of 400×, and Image-pro Plus 6.0 Image Analysis (Media Cybernetics) was used. The average optical density of the positive signal was analyzed by two investigators in a blinded manner.

Immunoblotting

Tissue samples were placed on ice and homogenized immediately with immunoprecipitation assay, cOmplete TM, Mini, EDTA-free Protease Inhibitor Cocktail and PhosSTOP TM phosphatase inhibitor tablets were added into Lysate buffer. Cell debris were pellet by centrifugation at 12,000 rpm, 4 °C for 10 min, protein concentrations were measured using the Bicinchoninic acid assay kit.

Equal amounts of protein samples (40 μg) were resolved by 4–12% sodium dodecyl sulfate–polyacrylamide gel electrophoresis (SDS-PAGE) and transferred into 0.45 μm polyvinylidene difluoride (PVDF) membranes. Membranes were in turn blocked with 5% nonfat dry milk or bovine-serum albumin (BSA) in 1X TBST (20 mM Tris–HCl, pH 7.6, 150 mM sodium chloride, 0.1% Tween-20) for 1 h in room temperature. The membranes were incubated with primary antibody for overnight at 4 °C with gentle shaking. After washing for 10 min in TBST with three cycles, the membranes were incubated with secondary antibody for 1 h at room temperature. Immunodetection was carried using Clarity TM Western ECL Substrate with the ChemiDoc XRS + Systems Gel Scanning Imager and Image Lab Gel Analysis System (BIO-RAD, Hercules, CA, USA).

Statistical analysis

SPSS 19.0 (IBM, Armonk, NY, USA) was used for statistical analysis. Measurement data conforming to a normal distribution are expressed as means ± SD. After testing for normality and homogeneity of variance, an analysis of variance by factorial design was used for comparisons. If the results showed an interaction between two factors, the simple main effect of each factor was analyzed. The Bonferroni method was used to correct the p value for multiple comparisons. Values of $p < 0.05$ were considered statistically significant.

Results

Hyperoxia-induced lung injury infant rats treated with OSI-027 achieved better general status and weight gain than treated with rapamycin

Infant SD rats in group A were full of spirit activity, ate well, exhibited normal growth and development, breathed smoothly, responded quickly to stimulation with clean and smooth body hair. Compared with group A, rats in group B showed low spirit, decreased activity, loss of appetite, slow reaction to stimulation, erect and messy body hair, shortness of breath, and slow gain in body weight. Compared with group B, rats in groups C and D showed a similar general status and slow weight gain on days 3 and 7. Compared to group C, group D had no difference in weight on days 3 and 7 (Table 1).

Hyperoxia-induced lung injury infant rats treated with OSI-027 achieved better general lung appearance than treated with rapamycin

The appearance of the lung at each time point in group A was generally normal. On day 7 in group B after hyperoxia intervention, the lungs became murky, grey, swollen, and less shiny, with scattered hemorrhagic spots. On day 14, the appearance of the lung was grayish-white, the swelling began to fade, and there were few bleeding points. Nodules of different sizes and cord-like grooves were observed on the local surface, and the lungs showed poor elasticity. Compared with B, groups C and D showed no obvious changes on day 3 and day 7. However, on day 14, group C showed more bleeding points, less elasticity, and more severe lung injury. Compared with B and C, group D had fewer focal hemorrhagic points, less hardness, better elasticity, and better lung appearance (Fig. 1a).

Table 1 Body weight statistics (g) (mean ± SD)

Group	A	B	C	D	*F*	*p*
Days 3 ($n=18$)	53.9 ± 3.6	46. 9 ± 2.5[a]	49.4 ± 2.4	48.2 ± 1.6	24.563	0.000
Days 7 ($n=12$)	79.6 ± 4.7	55.4 ± 3.4[a]	60.1 ± 6.9[a]	55.8 ± 4.1[a]	63.131	0.000
Days 14 ($n=6$)	117.2 ± 6.4	66.0 ± 5.6[a]	73.1 ± 3.3[ab]	65.6 ± 4.6[ac]	141.121	0.000
F	456.859	74.001	65.605	72.489	(p time = 573.426, $p=0.000$) (F group = 317.833, $p=0.000$) (F cross = 69.695, $p=0.000$)	
P	0.000	0.000	0.000	0.000		

Effects of rapamycin and OSI-027 on body weight in hyperoxy-induced lung injury infant rats. Group A: Normoxia + normal saline; B: Hyperoxia + normal saline; C: Hyperoxia + rapamycin; D: Hyperoxia + OSI-027

$p<0.05$

[a]Compared with group A

[b]Compared with group B

[c]Compared with group c

Hyperoxia-induced lung injury infant rats treated with OSI-027 achieved better histopathological performance than treated with rapamycin

Lung tissue structures were normal at all-time points in group A. Lung tissues in group B showed different degrees of injury. The alveolar septum thickened, and the structural disorder of lung tissues was gradually aggravated over time. On day 7, lung tissue inflammatory edema, alveolar septum thickening, and deformation reached a peak, and the alveoli collapsed within the lesion. By day 14, the inflammatory edema gradually subsided, but the alveolar septa were still thick, and the alveolar structures were destroyed. Increased collagen synthesis resulted in a pink precipitate in HE staining of pulmonary interstitial, and the fibrous tissues were characterized by cable-like scarring with a patchy distribution. There were obvious lung injury and fibrosis.

Compared with group B, the inflammation in the alveolar cavity and septum was more obvious in group C. Compared with groups B and C, inflammation and alveolar septum thickening were lower in group D, and lung injury and fibrosis were also alleviated (Fig. 1b).

Hyperoxia-induced lung injury infant rats treated with OSI-027 achieved better performance in lung *W/D*, alveolar septum thickness, and lung injury score than treated with rapamycin

Each index was included in an ANOVA. Time and group showed an interaction effect ($p<0.01$). According to the simple main effect, other than in group A, time influenced the lung *W/D*, alveolar septum thickness, and lung injury score ($p=0.001$). Compared with group A, *W/D* values in group B, C, and D increased on days 3 and 7 ($p<0.01$). Alveolar septum thickness and lung injury scores increased in group B on days 3, 7, and 14 ($p<0.01$). Compared with group B, group C had an increased alveolar septum thickness and lung injury score on days 7 and 14 ($p<0.01$), and in group D, the alveolar septum thickness and lung injury score were decreased ($p<0.01$) (Fig. 1c).

Hyperoxia activates mTOR signal pathway in infant rat lung tissue

The primary downstream targets of mTORC1 are p70S6 kinase 1 (p70S6K1) and eukaryotic initiation factor 4E binding protein 1 (4E-BP1), as well as the mTORC2 substrates, Akt (Ser473). Having established the role of mTOR signal pathway in hyperoxia-induced lung injury, We initially examined whether mTORC1/C2 signaling responded to hyperoxia in infant rat lung tissue. As shown in Fig. 2a, hyperoxia significantly increased the protein expression of mTOR, and the positive cells for mTOR were mainly distributed in the alveolar and bronchial epithelium, capillaries, and alveolar mesenchymal cells. Comparison of the normal ctrl versus hyperoxia on downstream mTOR substrates revealed that treatment with hyperoxia significantly increased phosphorylation of p70S6K, 4EBP1, and AKT, and more obvious with the increase of time (Fig. 2b).

Hyperoxia induces latent TGF-β1 activation in infant rat lung tissue, which contributes to TGF-β1-Smad signaling

Then we studied the effects of TGF-β1-Smad signaling, which was activated after treated with hyperoxia. TGF-β1 is produced in the form of latent complex and is activated by shedding the latency-associated protein (LAP)

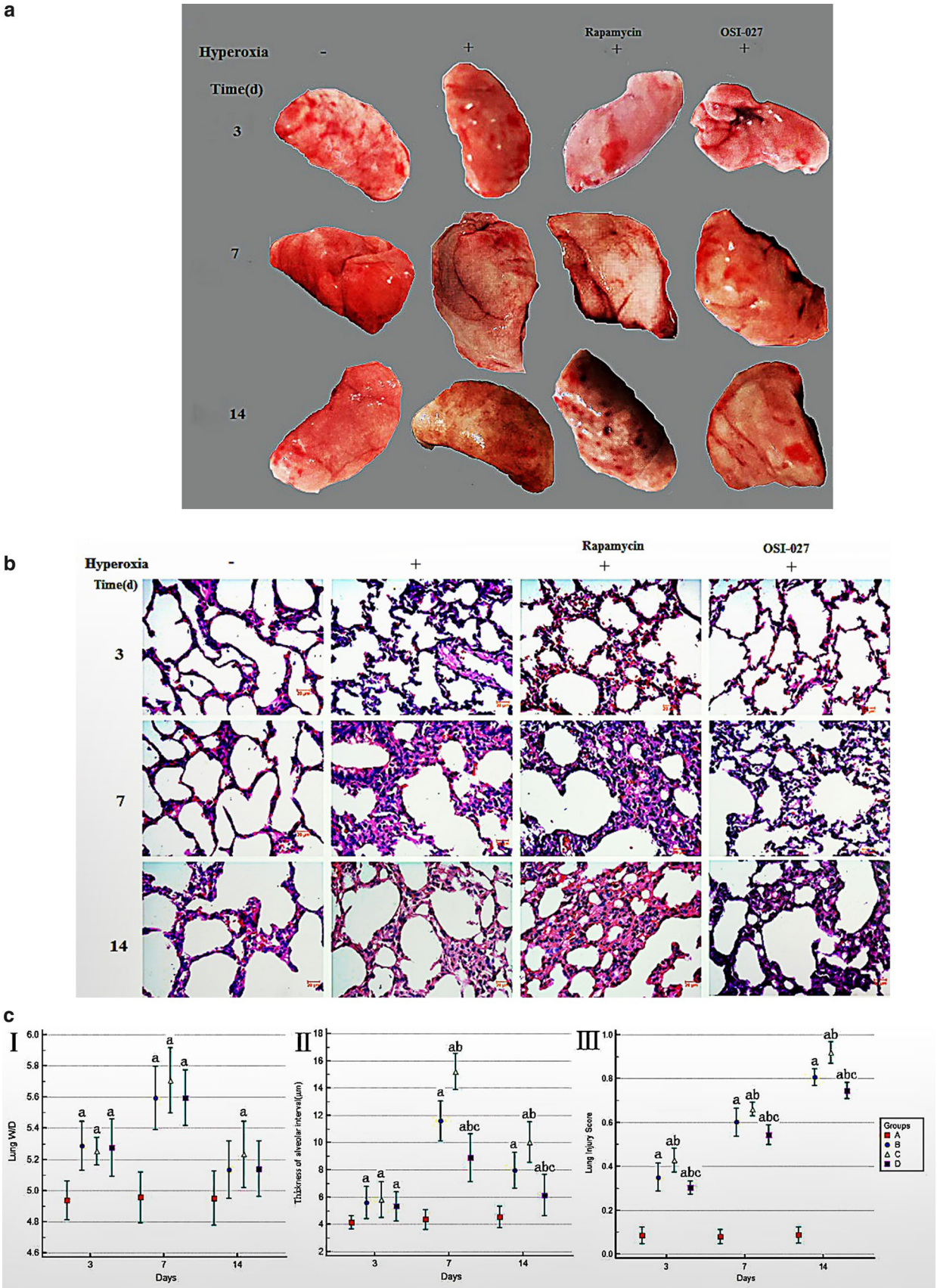
a
Hyperoxia
Time(d)
3
7
14
Rapamycin
OSI-027
b
c
I
II
III
Lung W/D
Thickness of alveolar interval(μm)
Lung Injury Score
Days
Groups
A
B
C
D

◂**Fig. 1** Hyperoxia-induced lung injury infant rats treated with OSI-027 achieved better performance in general lung appearance, histological observation and lung injury score than treated with rapamycin. **a** The lungs of infant rats treated with hyperoxia and hyperoxia plus rapamycin (1.5 mg kg^{-1} day^{-1}) every 2 days showed more bleeding points, less elasticity and more grayish colors obviously in 14 days. Conversely hyperoxia plus OSI-027 (0.5 mg kg^{-1} day^{-1}) every 2 days showed a better lung appearance. **b** Proliferation of alveolar cells, production of inflammatory fluid and cell, and collagen synthesis in groups treated with hyperoxia and hyperoxia plus rapamycin more apparently observed compared with which in ctrl and OSI-027 groups. **c** Infant rats with HILI treated with OSI-027(0.5 mg kg^{-1} day^{-1}) every 2 days showed better scores in lung wet/dry (I), alveolar septum thickness (II) and lung injury. (a: compare with Group A, b: compare with Group B, c compare with Group C; $p < 0.05$)

extracellularly or intracellularly, with this changing the latent form to trigger Smad signaling (Zhao et al. 2018). Previous studies have shown that activate latent TGF-β via a mechanism depends on ROS generation (Gonzalez-Gonzalez et al. 2017), so we investigated whether TGF-β1 activation by hyperoxia-induced ALI. Immunofluorescence showed that hyperoxia significantly increased the expression of TGF-β1 (Fig. 3a), so we next measured the dynamic balance change between LAP, TGF-β1 and TGF-β1, and the phosphorylation state of Smad2 and Smad3 of western immunoblotting. We found that hyperoxia treatment decreased latent TGF-β and increased active TGF-β in infant rat lung tissue (Fig. 3b), and the phosphorylation levels of Smad2 and Smad3 were elevated after treated with hyperoxia in a time-dependent manner (Fig. 3c).

Rapamycin attenuates the activity of mTORC1 signaling, and conversely, enhanced p-AKT and active TGF-β1 induction in infant rat lung tissue

Rapamycin performs its function through the inhibition of mTOR signaling. But current research shows that its role in lung injury and fibrosis is contradictory. Therefore, we studied the function of rapamycin, the partial allosteric mTORC1 inhibitor, on hyperoxia-induced mTOR signaling activation in infant rat lung tissue. As Fig. 4a revealed that treatment with rapamycin completely inhibited pS6K1 phosphorylation, whereas its effect on mTORC1-mediated 4E-BP1 (Thr37/46) phosphorylation was ineffective. Previous studies have uncovered that inhibition of mTOR results in Akt activation via a negative feedback loop begins at pS6K1 (O'Brien et al. 2014). To go one step further clarify rapamycin's regulatory effect on hyperoxia-induced ALI, we examined the phosphorylation of Akt and active TGF-β1 pathway in infant rat lung tissue under rapamycin treatment. As expected, rapamycin activated Akt and TGF-β1 signaling as indicated by phosphorylation of Akt and Smad2/Smad3 (Fig. 4b) and converting the latent form of TGF-β1 (Fig. 4c). These results suggested that rapamycin upregulated Akt and TGF-β1 signaling expression through the inactivation of mTORC1 signaling.

OSI-027 attenuates the activity of mTORC1/C2 signaling, which contributes to reduce hyperoxia-induced TGF-β1 activation in infant rat lung tissue

Having established a potential function for the Akt/TGF-β1 pathway, we next examined the contribution of mTOR signaling to HALI in infant rat lung tissue using OSI-027, the potent and highly selective ATP-competitive mTOR kinase inhibitors, that both mTORC1/2 are targeted. Hyperoxia-induced phosphorylation of the mTORC1 substrates, p70S6K (Thr389) and 4E-BP1 (Thr37/46, Ser65) significantly attenuated by OSI-027 in a time-dependent manner, as well as the mTORC2 substrates, Akt (Ser473) (Fig. 5a). The compound was also very effective in inhibiting the activation of TGF-β1 (Fig. 5b), and the corresponding inhibition of the phosphorylation of Smad2 and Smad3 caused by hyperoxia in infant rat lung tissue (Fig. 5c), suggesting that the mTOR/AKT/TGF-β1 signaling represents a common HALI pathway derived from infant rat lung tissue combined with the effects of rapamycin.

Discussion

The lungs of infants and children are most directly affected by prolonged oxygen treatment with high concentrations (Taha et al. 2016). Hyperoxia may cause irreversible damage to the structure and function of the lungs. We recently reported that mTOR inhibition attenuates HALI in infant rat lung tissue (Dang et al. 2017). We now analyze the relative contribution of activated mTOR to TGF-β1 signaling and show that mTORC2/AKT/TGF-β1 and mTORC1/4E-BP1 signaling with rapamycin-insensitive are critical for the hyperoxic response in infant rat lung tissue. Targeting mTOR by ATP-competitive mTORC1/C2 inhibition further significantly attenuates HALI in the infant rats.

In other experimental studies, it has been shown that exposure of the developing lung to high concentrations of oxygen inhibits the formation of alveoli and reduces the surface area of the lung, and the alveolar surface area and fibrosis scores were found to be significantly higher in HILI groups compared with control group (Özdemir et al. 2014, 2019). Like these studies, we developed a rat model of HILI. As expected, lung tissues in infant rats exhibited progressive inflammatory injury and fibrosis within 14 days of hyperoxic treatment, along with a worsening of the general state of

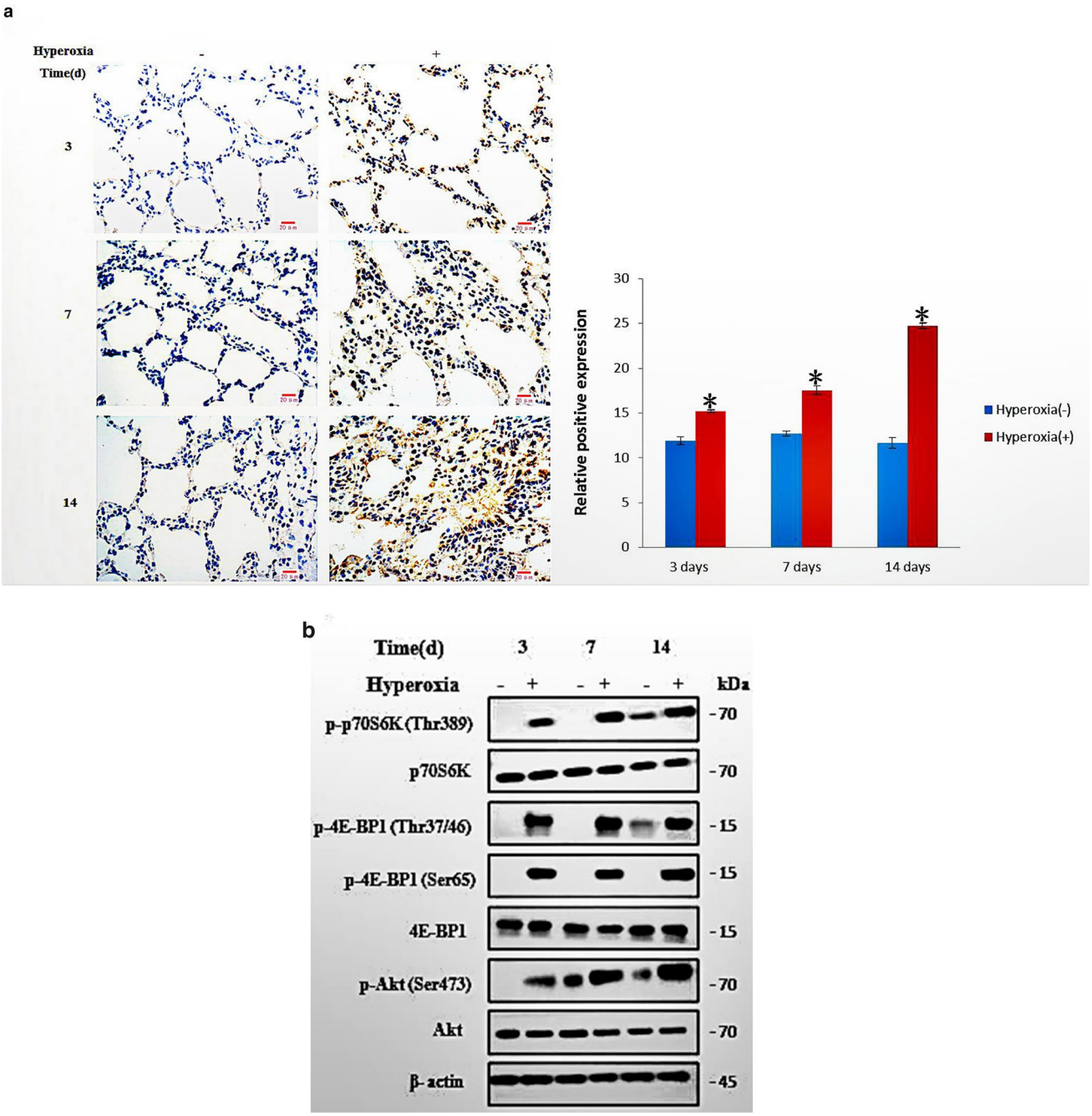

Fig. 2 **a** The lungs slides of hyperoxia-treated infant rats and ctrl rats were subjected to immunohistochemical staining with antibodies against mTOR, and positive cells were observed significantly in HILI in a time-dependent manner (*$p < 0.05$: compare with hyperoxia (−)). **b** Infant rats were treated with hyperoxia at indicated concentrations for 14 days. Lysates from lung tissue on days 3, 7, and 14 were subjected to Western blot analysis with antibodies against AKT1, p70S6K and 4EBP1, and their phosphorylation. β-Actin was used as a loading control

infant rats. On day 14 of the hyperoxic treatment, the lung injury score was significantly increased, and hyperplasia of the lung interstitium and fibroblasts already appeared.

mTOR functions as a serine/threonine–protein kinase that regulates cell growth, cell proliferation, cell motility, cell survival, protein synthesis, autophagy, and transcription. It is commonly expressed in respiratory epithelium and lung tissue and previous studies have demonstrated that mTOR plays a pivotal role in acute injury, inflammation and fibrosis of lung (Mitani et al. 2016; Hsu et al. 2017). In this study, we initially found that hyperoxia activated mTOR signaling in infant rats injured-lung tissue by phosphorylation of the

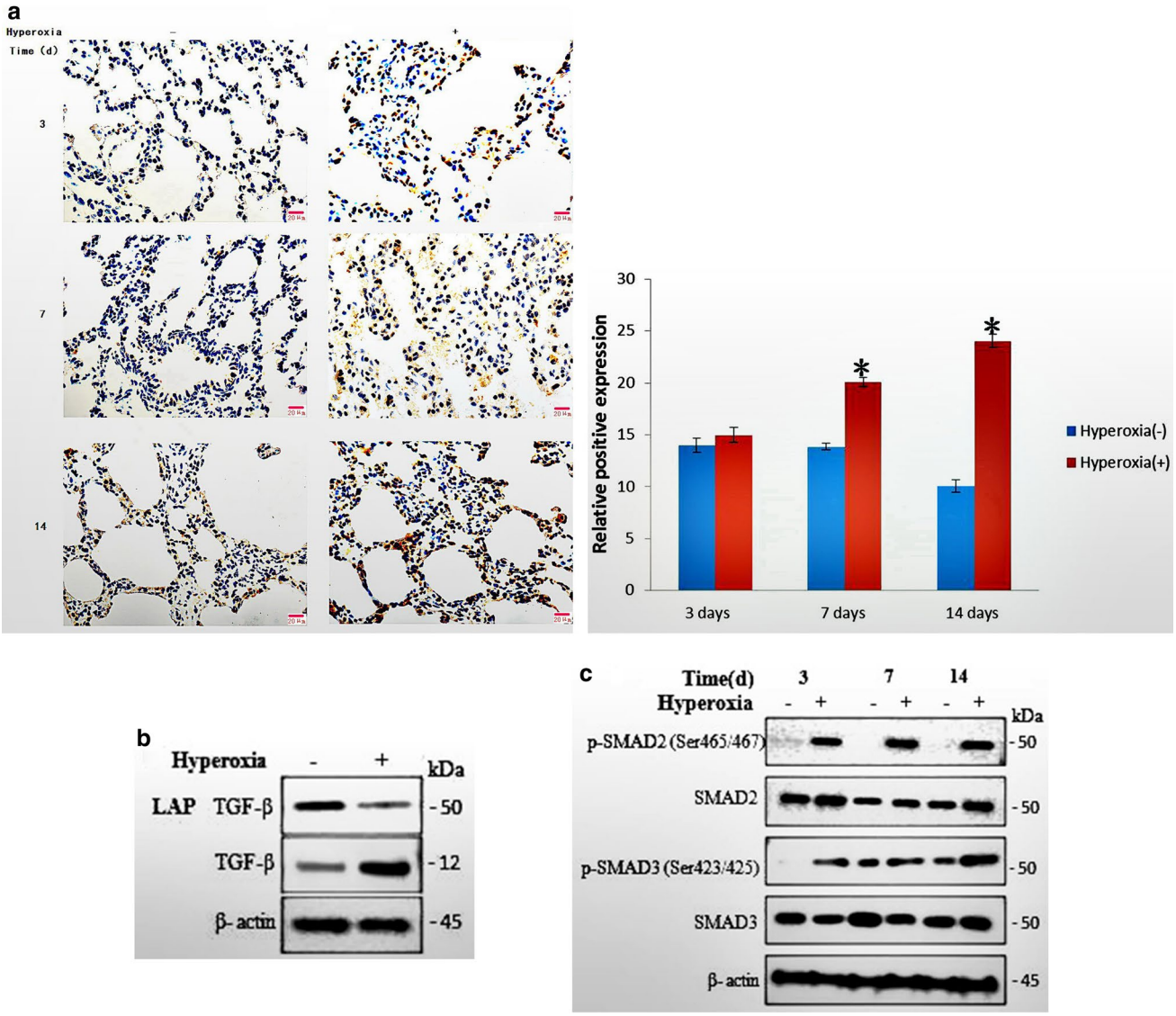

Fig. 3 **a** The lungs slides of hyperoxia-treated infant rats and ctrl rats were subjected to immunohistochemical staining with antibodies against TGF-β1, and positive cells were observed significantly in HILI in a time-dependent manner (*$p < 0.05$: compare with hyperoxia (−)). **b** Infant rats were treated with hyperoxia at indicated concentrations for 14 days. Lysates from lung tissue on days 3, 7, and 14 were subjected to Western blot analysis with antibodies against latent TGF-β and active TGF-β. β-Actin was used as a loading control. **c** Lysates from lung tissue of HILI on days 3, 7, and 14 were subjected to Western blot analysis with antibodies against Smad2/3, and their phosphorylation. β-Actin was used as a loading control

p70S6 kinase 1 (p70S6K1) and eukaryotic initiation factor 4E binding protein 1 (4E-BP1) (primary downstream targets of mTORC1), as well as the substrates Akt (Ser473) of mTORC2.

In a further pursuit to uncover the potential mechanisms for HILI in infant rats, we found an activation of TGF-β1-Smad2/3 signaling. Transforming growth factor β1 encoded protein regulates cell proliferation, differentiation and growth, and can modulate expression and activation of other growth factors. It is considered as the main cytokine of inflammation and fibrogenesis (Bonniaud et al. 2005). Some previous studies have shown that TGF-β1 was mainly induced by mTOR in pneumonia and pulmonary fibrosis (Racanelli et al. 2018), and it also up-regulated the expression of TGF-β1 in many cell types including lung epithelium and interstitial cells (Koh et al. 2016). Strongly suggesting that maybe TGF-β1-Smad signaling was involved in hyperoxia-induced mTOR signaling activation in infant rats lung tissue. In the present study, our experiments revealed that TGF-β1 protein increased immunohistochemically after treatment with hyperoxia in a time-dependent manner. The results also indicated that treatment with hyperoxia

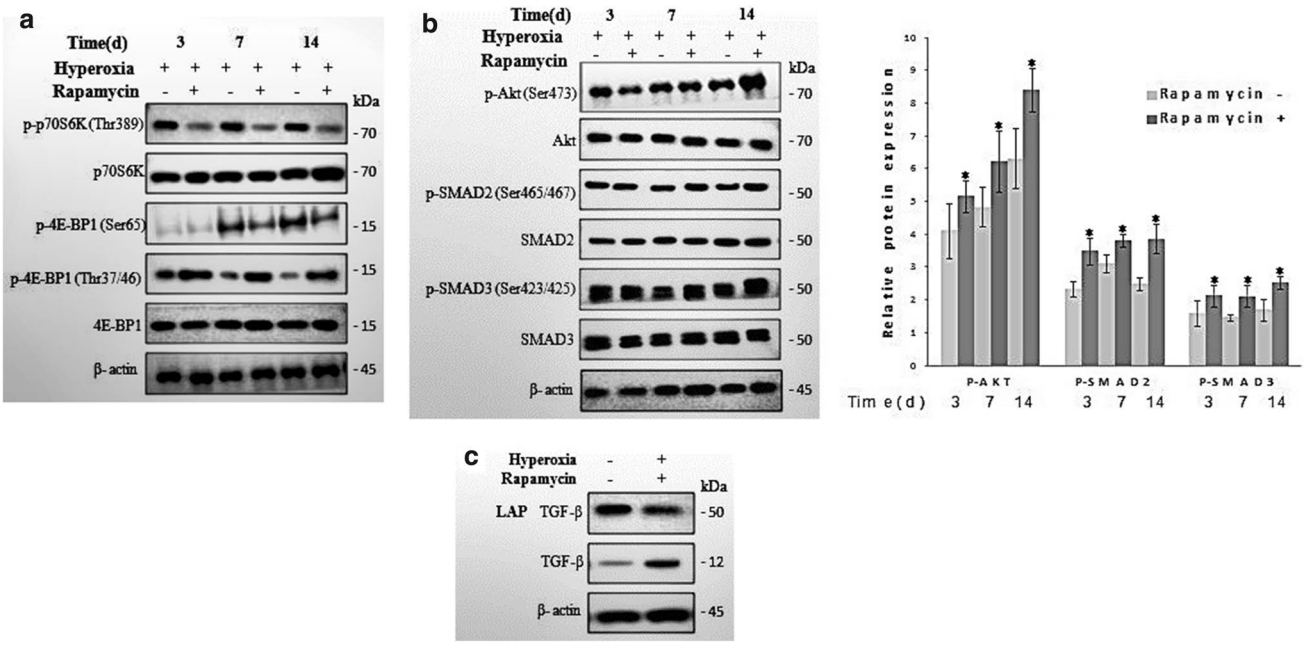

Fig. 4 HILI Infant rats were treated with rapamycin at indicated concentrations for 14 days, and HILI Infant rats were used as ctrl group. **a** Lysates from lung tissue on days 3, 7, and 14 were subjected to Western blot analysis with antibodies against p70S6K and 4EBP1, and their phosphorylation. **b** Lysates from lung tissue on days 3, 7, and 14 were subjected to Western blot analysis with antibodies against AKT1 and Smad2/3, and their phosphorylation. β-Actin was used as a loading control (*$p < 0.05$: compare with rapamycin (−)). **c** Lysates from lung tissue on days 3, 7, and 14 were subjected to Western blot analysis with antibodies against latent TGF-β and active TGF-β

increased active TGF-β and decreased latent TGF-β in HILI, and Smad2 and Smad3 were elevated in which phosphorylation levels. Previous studies demonstrated that prolonged exposure to hyperoxia leads to the generation of excessive reactive oxygen species (ROS) (Zaher et al. 2007), which can induce oxidation on specific amino acids in LAP, triggering conformational changes, allowing the rapid release of TGF-β. Ours results are consistent with those reports, and the mechanism of whether hyperoxia triggers intracellular ROS formation in HILI or by other ways besides this to activate TGF-β1 still needs further investigation.

To identify the potential mechanism by which mTOR whether and how influences the TGF-β1 activation response in HILI, We consequently added our analysis to explore the impact of mTORC1 and mTORC1/C2 inhibition on TGF-β1-Smad2/3 signaling to HILI by comparing the effect of rapamycin with OSI-027. Our pathological observation and proteomics research reveals significant differences between the two compounds in both anti-HILI potential and activation of TGF-β1 signaling: in addition to achieve better general status, weight gain and lung appearance in hyperoxia-treated infant rats, OSI-027 also alleviated other major histological performance of the inflammation and fibrosis including alveolar wall hyperplasia and deformation, inflammatory exudation, and fibroblast formation. These results may have a close causal relationship: because OSI-027 improves the inflammation and fibrosis of the alveolar cells of hyperoxia-treated infant rats, further improves the general status of the rats. In contrast, these pathological damages induced by hyperoxia were completely rapamycin-insensitive and even worse.

Our data further provided evidence for the involvement of the target pathway, as the anti-HILI effect of OSI-027 was related to the inhibition of mTORC1 substrates [p70S6K (Thr389) and 4E-BP1 (Thr37/46)] and same with mTORC2 substrate, Akt1 phosphorylation, and reduced the activation of TGF-β1-Smad2/Smad3 signaling. These results are consistent with the effects of OSI-027 on mTOR1/2 and TGFβ1 in other research fields, such as scar formation and tumor development (Huang et al. 2018; Wang et al. 2020). Conversely, rapamycin is an allosteric inhibitor compared to this ATP-competitive mTOR inhibitor that directly binds to the mTOR catalytic site, binding only to the FKBP12/rapamycin binding (FRB) domain of mTORC1 to restrict the substrate is close to the catalytic site. Our phosphoproteomics studies have shown that mTORC1 substrates p70S6K and 4E-BP1 have different sensitivities to rapamycin treatment. p70S6K (Thr389) was readily sensitive to rapamycin treatment and weakly phosphorylated, whereas 4E-BP1 (Thr37/46) was insensitive to rapamycin treatment and avidly phosphorylated. In addition, rapamycin also activates phosphorylation of AKT and induce the activation of TGF-β1, which

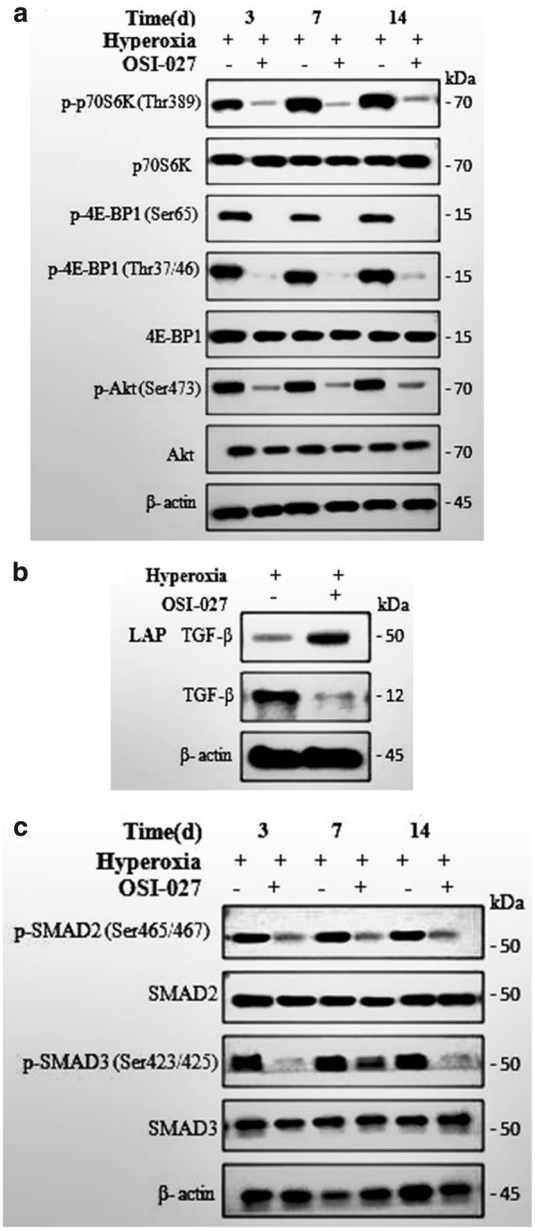

Fig. 5 HILI Infant rats were treated with OSI-027 at indicated concentrations for 14 days, and HILI Infant rats were used as ctrl group. **a** Lysates from lung tissue on days 3, 7, and 14 were subjected to Western blot analysis with antibodies againstAKT1, p70S6K and 4EBP1, and their phosphorylation. **b** Lysates from lung tissue on days 3, 7, and 14 were subjected to Western blot analysis with antibodies against latent TGF-β and active TGF-β. **c** Lysates from lung tissue on days 3, 7, and 14 were subjected to Western blot analysis with antibodies against Smad2/3, and their phosphorylation. β-Actin was used as a loading control

is closely related to the negative reflection of weakly phosphorylated p70S6K (Kang et al. 2013) and a special cellular environment.

Conclusions

Our data provide the support that mTOR mediates the HILI effect in infant rats via a mTORC2/AKT/TGF-β1 and a rapamycin-insensitive mTORC1/4E-BP1 signaling.

Analysis of the opposite effects of rapamycin and OSI-027 on HILI indicate that rapamycin attenuates 4E-BP1 (Ser65) phosphorylation alone is not sufficient to block mTORC1-mediated HILI effects and further shows that the significant effect of competitive mTORC1/C2 on HILI maybe mediated by a potent inhibitory effect on the phosphorylation of mTOR/AKT/TGF-β1 and mTORC1/4E-BP1 (Thr37/46) signaling.

Acknowledgements This study was supported by a Grant from the Basic And Frontier Research Project From Chongqing Science And Technology Commission, Chongqing, China (cstc2018jcyjAX0046).

Author contributions Conceptualization, writing-review, and editing: HD and LL; Data curation and investigation: LL and ML; Formal analysis, funding acquisition, methodology and software: HD, PW, LL, YL, ML; Writing-original draft: HD; Project administration: HD; Resources and visualization: LL, ML. Supervision: HD; Validation: LL and ML.

Declarations

Conflict of interest The authors have declared that no conflict of interest exists.

Ethical approval All animal experiments were performed with local ethical committee approval (Ethics Committee of Chongqing Medical University, Chongqing, China). This study also followed the National Institutes of Health guide for the care and use of Laboratory Animals (NIH Publications No. 8023, revised 1978).

References

Andreollo NA, de Santos EF, Araújo MR, Lopes LR (2012) Rat's age versus human's age: what is the relationship? Arq Bras Cir Dig 25:49–51

Bahrami A, Khazaei M, Hasanzadeh M, ShahidSales S, Joudi Mashhad M, Farazestanian M et al (2018) Therapeutic potential of targeting PI3K/AKT pathway in treatment of colorectal cancer: rational and progress. J Cell Biochem 119:2460–2469

Bonniaud P, Margetts PJ, Ask K, Flanders K, Gauldie J, Kolb M (2005) TGF-beta and Smad3 signaling link inflammation to chronic fibrogenesis. J Immunol 175:5390–5395

Dang H-X, Li J, Liu C, Fu Y, Zhou F, Tang L et al (2017) CGRP attenuates hyperoxia-induced oxidative stress-related injury to alveolar epithelial type II cells via the activation of the Sonic hedgehog pathway. Int J Mol Med 40:209–216

Dejust S, Morland D, Bruna-Muraille C, Eymard J-C, Yazbek G, Savoye A-M et al (2018) Everolimus-induced pulmonary toxicity: findings on 18F-FDG PET/CT imaging. Medicine (Baltimore) 97:e12518

Gonzalez-Gonzalez FJ, Chandel NS, Jain M, Budinger GRS (2017) Reactive oxygen species as signaling molecules in the development of lung fibrosis. Transl Res 190:61–68

Gupta M, Hendrickson AEW, Yun SS, Han JJ, Schneider PA, Koh BD et al (2012) Dual mTORC1/mTORC2 inhibition diminishes Akt activation and induces Puma-dependent apoptosis in lymphoid malignancies. Blood 119:476–487

Hamdani S, Thiolat A, Naserian S, Grondin C, Moutereau S, Hulin A et al (2017) Delayed and short course of rapamycin prevents organ rejection after allogeneic liver transplantation in rats. World J Gastroenterol 23:6962–6972

Helmerhorst HJF, Roos-Blom M-J, van Westerloo DJ, de Jonge E (2015) Association between arterial hyperoxia and outcome in subsets of critical illness: a systematic review, meta-analysis, and meta-regression of cohort studies. Crit Care Med 43:1508–1519

Higgins RD, Jobe AH, Koso-Thomas M, Bancalari E, Viscardi RM, Hartert TV et al (2018) Bronchopulmonary dysplasia: executive summary of a workshop. J Pediatr 197:300–308

Hsu H-S, Liu C-C, Lin J-H, Hsu T-W, Hsu J-W, Su K et al (2017) Involvement of ER stress, PI3K/AKT activation, and lung fibroblast proliferation in bleomycin-induced pulmonary fibrosis. Sci Rep 7:14272

Hu Y, Liu J, Wu Y-F, Lou J, Mao Y-Y, Shen H-H et al (2014) mTOR and autophagy in regulation of acute lung injury: a review and perspective. Microbes Infect 16:727–734

Huang S, Yang C, Li M, Wang B, Chen H, Fu D et al (2018) Effect of dual mTOR inhibitor on TGFβ1-induced fibrosis in primary human urethral scar fibroblasts. Biomed Pharmacother 106:1182–1187

Kallet RH, Matthay MA (2013) Hyperoxic acute lung injury. Respir Care 58:123–141

Kang SA, Pacold ME, Cervantes CL, Lim D, Lou HJ, Ottina K et al (2013) mTORC1 phosphorylation sites encode their sensitivity to starvation and rapamycin. Science 341:1236566

Koh HB, Scruggs AM, Huang SK (2016) Transforming growth factor-β1 increases DNA methyltransferase 1 and 3a expression through distinct post-transcriptional mechanisms in lung fibroblasts. J Biol Chem 291:19287–19298

Mitani A, Ito K, Vuppusetty C, Barnes PJ, Mercado N (2016) Restoration of corticosteroid sensitivity in chronic obstructive pulmonary disease by inhibition of mammalian target of rapamycin. Am J Respir Crit Care Med 193:143–153

Nadon AM, Perez MJ, Hernandez-Saavedra D, Smith LP, Yang Y, Sanders LA et al (2014) Rtp801 suppression of epithelial mTORC1 augments endotoxin-induced lung inflammation. Am J Pathol 184:2382–2389

O'Brien NA, McDonald K, Tong L, von Euw E, Kalous O, Conklin D et al (2014) Targeting PI3K/mTOR overcomes resistance to HER2-targeted therapy independent of feedback activation of AKT. Clin Cancer Res 20:3507–3520

Ošt'ádalová I, Babický A (2012) Periodization of the early postnatal development in the rat with particular attention to the weaning period. Physiol Res 61:S1–S7

Özdemir ÖMA, Gözkeser E, Bir F, Yenisey Ç (2014) The effects of resveratrol on hyperoxia-induced lung injury in neonatal rats. Pediatr Neonatol 55:352–357

Özdemir ÖM, Taban Ö, Enli Y, Bir F, Şahin B, Ergin H (2019) The effects of bosentan on hyperoxia-induced lung injury in neonatal rats. Pediatr Int 61:1120–1126

Racanelli AC, Kikkers SA, Choi AMK, Cloonan SM (2018) Autophagy and inflammation in chronic respiratory disease. Autophagy 14:221–232

Reyburn B, Martin RJ, Prakash YS, MacFarlane PM (2012) Mechanisms of injury to the preterm lung and airway: implications for long-term pulmonary outcome. Neonatology 101:345–352

Segura-Ibarra V, Amione-Guerra J, Cruz-Solbes AS, Cara FE, Iruegas-Nunez DA, Wu S et al (2017) Rapamycin nanoparticles localize in diseased lung vasculature and prevent pulmonary arterial hypertension. Int J Pharm 524:257–267

Taha DK, Kornhauser M, Greenspan JS, Dysart KC, Aghai ZH (2016) High flow nasal cannula use is associated with increased morbidity and length of hospitalization in extremely low birth weight infants. J Pediatr 173:50–55

Tian T, Li X, Zhang J (2019) mTOR signaling in cancer and mTOR inhibitors in solid tumor targeting therapy. Int J Mol Sci 20:755

Vogel ER, Britt RD, Trinidad MC, Faksh A, Martin RJ, MacFarlane PM et al (2015) Perinatal oxygen in the developing lung. Can J Physiol Pharmacol 93:119–127

Wang H, Liu Y, Ding J, Huang Y, Liu J, Liu N et al (2020) Targeting mTOR suppressed colon cancer growth through 4EBP1/eIF4E/PUMA pathway. Cancer Gene Ther 27:448–460

Yang H, Jiang X, Li B, Yang HJ, Miller M, Yang A et al (2017) Mechanisms of mTORC1 activation by RHEB and inhibition by PRAS40. Nature 552:368–373

Zaher TE, Miller EJ, Morrow DMP, Javdan M, Mantell LL (2007) Hyperoxia-induced signal transduction pathways in pulmonary epithelial cells. Free Radic Biol Med 42:897–908

Zhao B, Xu S, Dong X, Lu C, Springer TA (2018) Prodomain-growth factor swapping in the structure of pro-TGF-β1. J Biol Chem 293:1579–1589